JOURNAL OF Materials CHEMISTRY

# Correlation of friction, adhesion, wettability and surface chemistry after argon plasma treatment of poly(ethylene terephthalate)

**Ben D. Beake,[a] John S. G. Ling[b] and Graham J. Leggett*[a]**

[a]*Department of Chemistry, The University of Manchester Institute of Science and Technology, PO Box 88, Manchester, UK M60 1QD*
[b]*British Steel, Welsh Technology Centre, Port Talbot, West Glamorgan, UK SA13 2NG*

***Received 17th September 1998, Accepted 12th October 1998***

The combination of wettability, X-ray photoelectron spectroscopy and scanning force microscopy has been used to analyse the changes to the surface after plasma treatment of poly(ethylene terephthalate) film. Calculations on contact angle data with a combination of polar and non-polar liquids have shown that argon plasma treatment considerably enhances the work of solid–(polar) liquid adhesion and the surface free energy of the films due to the creation of acidic and basic functions on the polymer surface. In contrast, Lifshitz–van der Waals (apolar) interactions decrease slightly as a consequence of plasma-induced chain-scission. We present the first study of a plasma-treated polymer by chemical force microscopy. Plasma-modified surfaces exhibit substantially higher friction than untreated material and are more easily disrupted by the movement of the tip during scanning. Friction is reduced when methyl-functionalised tips are employed. There is a correlation, on plasma treatment, between the rapid increases in surface friction probed by lateral force microscopy and surface free energy probed by wettability and X-ray photoelectron spectroscopy. The modified mechanical properties and polar group incorporation both result from scission of polymer chains and contribute to the lateral force contrast.

## Introduction

The control of the chemical, mechanical and topographical properties of surfaces is relevant in numerous applications of polymers in the textiles, adhesives, composites and coatings industries.[1–6] Many of these applications require good adhesion between the polymer and a surface coating. Plasma treatment is an effective method for improving the bondability and wettability of polymer surfaces whilst leaving bulk properties unaltered. In a plasma the surface is exposed to a broad spectrum of ions, electrons, excited neutrals, radicals, UV and VUV radiation.[2,7] The predominant reactive species in an inductively coupled radio frequency argon plasma are thought to be argon ions and VUV photons which produce excited states at the surface, the decay of which leads to the formation of radicals.[2,6,7]

We have previously investigated the relationship between changing wettability and surface morphology under different plasma conditions.[8] Completely hydrophilic surfaces were not obtained even after several hours treatment. Wettability is thought to be limited by competition between etching of the surface (*via* chain scission) and chemical functionalisation (incorporation of polar groups).[8–10] Scanning force microscopy (SFM), imaging in an intermittent contact mode, where the tip taps the surface, showed that the formation of orientated, ridged surface structures occurred over an extended time scale.[8]

In this paper we aim to analyse the changes to surface chemistry further and investigate their role in surface friction. Our objective is the development of SFM-based technologies for exploring the nanoscale properties of polymer surfaces that have been modified in plasma. We were interested to know whether there was a correlation between changes in wettability and the frictional properties of the modified polymer surface. It is known that acid–base (electron donor–acceptor) chemistry plays an important role in the interfacial interactions of polymers, significantly improving their mixing, adhesion, adsorption on fillers and fibres and their solubility in organic liquids.[11] Specifically, we have shown how it is possible to calculate the surface free energy of poly(ethylene terephthalate) [PET] and the thermodynamic work of adhesion between the surface and polar liquids, and have determined the effect of different plasma treatment conditions on these quantities. X-Ray photoelectron spectroscopy has been used to investigate the compositional changes in the surface/near-surface region that are responsible for the improvement in wettability after exposure to argon plasma. The level of oxygen incorporation with increasing time of argon plasma treatment provides a means to monitor the extent of surface functionalisation.

Recently, scanning force microscopy has been used to examine the changes to surface topography which occur on plasma treatment of polymers such as polytetrafluoroethylene,[12] polypropylene,[13,14] polymethylmethacrylate[15] and poly(ethylene terephthalate) (PET).[8] In addition to the topographical information, by operating the scanning force microscope in lateral (or frictional) force mode the effects of the plasma modification on the nanoscale surface properties of the polymer can be investigated. In lateral force microscopy (LFM), the torsional or twisting motions of the cantilever are recorded with high contrast, and are regarded as being indicative of frictional interactions between tip and sample.[16] The difference in the lateral force signal between forward and reverse scans is proportional to the friction force during imaging.[16,17] This friction is thought to correlate with adhesion since on the molecular scale both processes involve bond breaking and formation.[18] In order to investigate the effect of tip–sample chemical interactions on the friction force, we have used chemical force microscopy (CFM), in which the tip chemistry is controlled by the deposition of a self-assembled monolayer (SAM). To our knowledge this is the first study of a plasma treated polymer by CFM. We hypothesised that if the increase in friction on plasma-treatment is predominantly the result of increased acid–base interactions between tip and sample then the measured friction force should vary with tip chemistry in the following order: acid-terminated tip > uncoated silicon nitride tip > methyl-terminated tip and the magnitude of the increase in friction on plasma treatment should be significantly lower when the apolar, methyl-functionalised tips are used.

## Experimental

Melinex 'O', an additive-free PET with low surface roughness, was obtained from ICI (Wilton, UK). Mylar D (manufactured by Du Pont, USA), a PET film treated to incorporate a particulate silicate surface additive, was obtained from Goodfellow Advanced Materials (Cambridge, UK). Both materials were biaxially orientated and were used as received.

Plasma treatments were carried out in an inductively-coupled radio frequency (13.56 MHz) reactor with a base pressure of $4 \times 10^{-2}$ mbar, constructed following a design by Dr R. D. Short of the Department of Engineering Materials at the University of Sheffield. Argon (BOC, special gases, UK) was flowed through the reactor for 15 min before treatment. Plasma treatment was carried out at 0.1 or 1.0 mbar argon pressure and 10 W power. After treatment, the reactor was evacuated down to base pressure before exposing the sample to laboratory atmosphere.

Static advancing contact angles were measured within 30 minutes of plasma treatment on a Rame–Hart model 100-00 goniometer. Water was triply distilled before being passed through a Millipore 'Milli-Q' purification system. Diiodomethane (>99%), 1-bromonaphthalene (>97%), formamide (>99.5%), glycerol (>99.5%), and ethylene glycol (>99.5%) were all from Merck (Darmstadt, Germany) and used as supplied. Recorded angles are averages of at least six measurements.

X-Ray photoelectron spectra of PET samples treated with argon plasma at 0.1 mbar were recorded using a Vacuum Generators ESCALAB instrument with a base pressure of $1 \times 10^{-8}$ mbar. The system was equipped with an unmonochromated twin anode X-ray source and 100 mm radius hemispherical electron energy analyser. The sample area analysed by this system was approximately 9 mm in diameter with a take-off angle of 60°. Al-K$\alpha$ radiation (1486.6 eV) was used throughout. Survey scans (at 50 eV analyser pass energy) and C 1s and O 1s scans (at 10 eV pass energy) were recorded. The areas under C 1s and O 1s curves were calculated and the O:C ratios were determined using empirically derived sensitivity factors reported by Briggs and Seah.[19]

Topographic scanning force microscopy (SFM) images were obtained in ambient conditions with a TopoMetrix Explorer scanning probe microscope (TopoMetrix Corp., Saffron Walden, UK). Contact mode imaging was generally performed using silicon nitride cantilevers (nominal force constant 0.064 N m$^{-1}$) supplied by the microscope manufacturer. The only exception was for the CFM data where Nanoprobes (nominal force constant 0.12 N m$^{-1}$, from Digital Instruments) were used. The applied load was thought to be <10 nN for the contact mode imaging in constant force mode. Lateral force imaging was performed simultaneously with the topographical imaging. The effect of scan velocity on the observed lateral force contrast has been documented.[20,21] Since we are only interested in relative changes to the frictional force signal, this complication has been avoided by acquiring all scans in Fig. 7–10 at a constant scan rate (21 μm s$^{-1}$). To allow meaningful comparison of the frictional responses of different materials, the same tip was used throughout, and the alignment of the laser on the cantilever was not altered for all of the samples tested. The lateral force signals on line profiles from the forward and reverse lateral force images were compared to produce friction loops.

A Nanoscope IIIa MultiMode AFM (Digital Instruments, UK) was used for the chemical force microscopy study. The scope mode of the microscope was utilised to provide friction loops. 'Nanoprobe' SFM tips were modified[18] with alkanethiol SAMs of the same carbon chain length terminated with either hydrophilic (carboxylic acid) groups or hydrophobic (methyl) groups. A General Engineering bell jar vacuum system was used to coat the tip-cantilever assemblies, as follows: (a) 2 nm of Cr and 20–25 nm of Au on the front face, and (b) 18–20 nm of Au on the back-face of the cantilever. The evaporation rate for the gold was always below 0.03 nm s$^{-1}$ to ensure that the cantilevers did not bend during heating.[18,22] Once cool, the cantilevers were immersed in 1 mM solutions of dodecanethiol (from Fluka) or mercaptoundecanoic acid in degassed ethanol for at least 18 h for the self-assembly process. The mercaptoundecanoic acid was synthesised according a procedure adapted from the literature.[23] All glassware was cleaned with 'Piranha' solution (3:7 mixture of 30% hydrogen peroxide and concentrated sulfuric acid) before use. (Great care should be exercised in handling Piranha solution; it is an extremely strong oxidising agent and has been known to detonate spontaneously on contact with organic material.) The functionalised tips were kept in the alkanethiol solutions until use.

## Results

### Contact angle goniometry

The observed contact angles of water, ethylene glycol, formamide, diiodomethane and glycerol on Melinex 'O' treated in 0.1 and 1.0 mbar argon plasmas are shown in Fig. 1 and 2 respectively. Increasing plasma treatment led to increasing wettability of the polymer by all the polar liquids. Near-limiting values at 0.1 and 1.0 mbar were obtained after 120 and 300 s respectively. In contrast, the contact angle of the apolar liquid diiodomethane was found to increase on short time exposure to plasma. Diiodomethane has a slight $\gamma^+$ component, but as a first approximation this liquid may be considered apolar.[24] We have found the inclusion or exclusion of this small polar term makes no difference to the surface

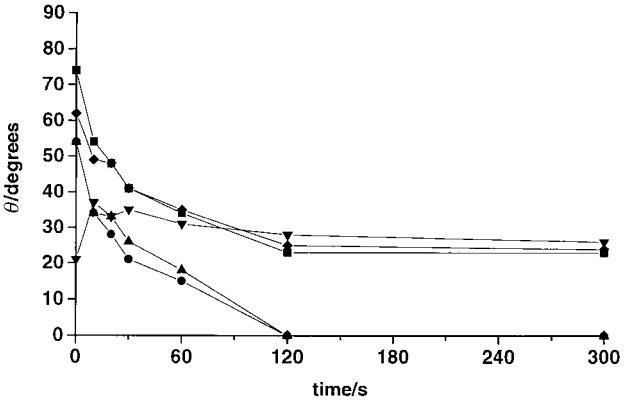


**Fig. 1** Contact angles of water (■), ethylene glycol (●), formamide (▲), diiodomethane (▼) and glycerol (◆) on PET plasma modified in 0.1 mbar argon.

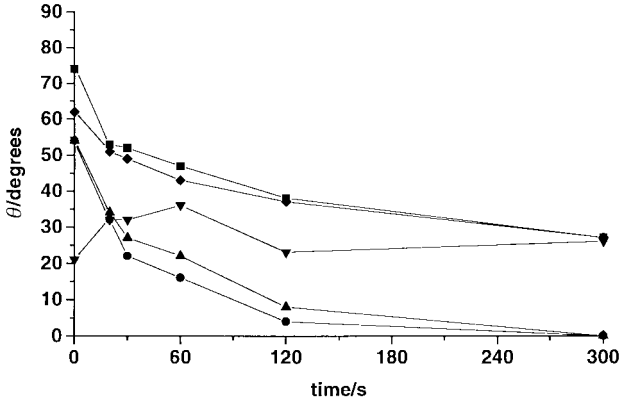


**Fig. 2** Contact angles of water (■), ethylene glycol (●), formamide (▲), diiodomethane (▼) and glycerol (◆) on PET plasma modified in 1.0 mbar argon.

energy calculations. Similar behaviour was also observed using another apolar liquid, 1-bromonaphthalene. There is close similarity between water and glycerol angles.

The contact angles of the five liquids shown in Fig. 1 and 2 have been used in the determination of the surface free energy change on argon plasma treatment using computer programs[25] following the method of van Oss *et al.*, using their values[24,26,29] for the surface tension parameters of the five liquids. Details of the calculation of surface free energy from contact angle data are given in Appendix 1. The change in surface free energy after plasma treatment at 0.1 and 1.0 mbar argon is shown in Fig. 3 and 4. A significant increase in the polar component can be clearly seen, with changes occurring faster at the lower pressure studied. Fig. 3 and 4 also show that at both argon pressures, the apolar component initially decreases on exposure to the plasma before recovering to a value near that on untreated Melinex 'O'. The increase in basic component to the surface free energy after plasma treatment is larger at either pressure studied than the increase in acidic component. The variation in the thermodynamic work of solid–liquid adhesion with treatment time has also been calculated. Fig. 5 illustrates the changes at 0.1 mbar for water and formamide.

### X-Ray photoelectron spectroscopy

An O:C ratio of $0.39 \pm 0.02$ was determined for untreated Melinex 'O' in good agreement with the theoretical value of 0.40. Fig. 6 shows C 1s spectra (corrected for charging effects) for untreated and plasma treated Melinex 'O'. The data show broadening of the line widths of the C 1s peaks. Similar behaviour has been reported in the XP C 1s spectra of several polymers, including PET, after argon plasma treatment, and is regarded as evidence of an increased variety of carbon species on plasma treatment.[7] Notably, a new peak has

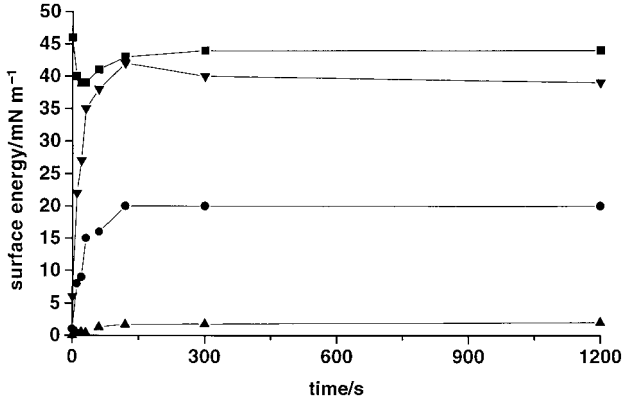


**Fig. 3** Surface free energy change on plasma treatment at 0.1 mbar argon; $\gamma_s^{LW}$ (■), $\gamma_s^{AB}$ (▼), $\gamma^+$ (▲) and $\gamma^-$ (●).

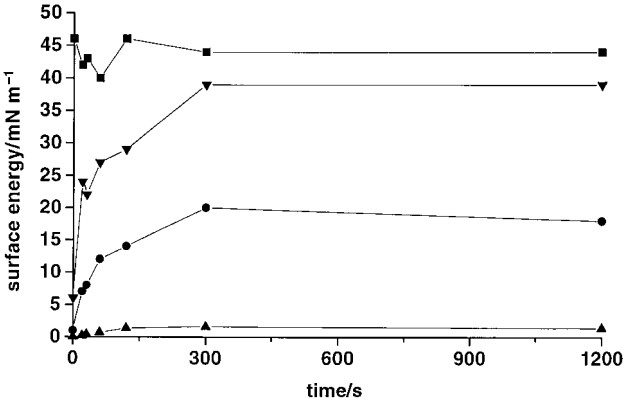


**Fig. 4** Surface free energy change on plasma treatment at 1.0 mbar argon; $\gamma_s^{LW}$ (■), $\gamma_s^{AB}$ (▼), $\gamma^+$ (▲) and $\gamma^-$ (●).

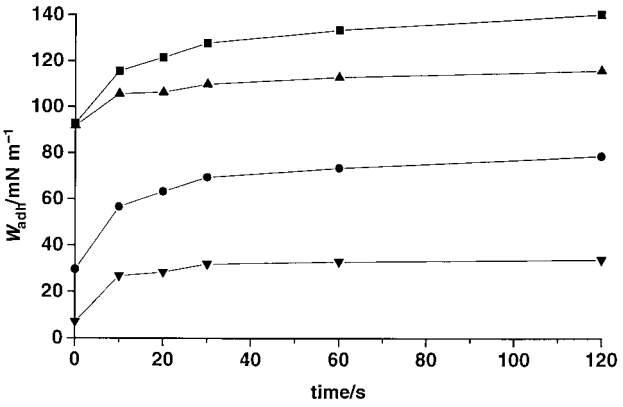


**Fig. 5** Thermodynamic work of polymer–water (■) and polymer–formamide (▲) adhesion after plasma treatment at 0.1 mbar. The acid–base components to the total work of adhesion are also shown; water (●) and formamide (▼).

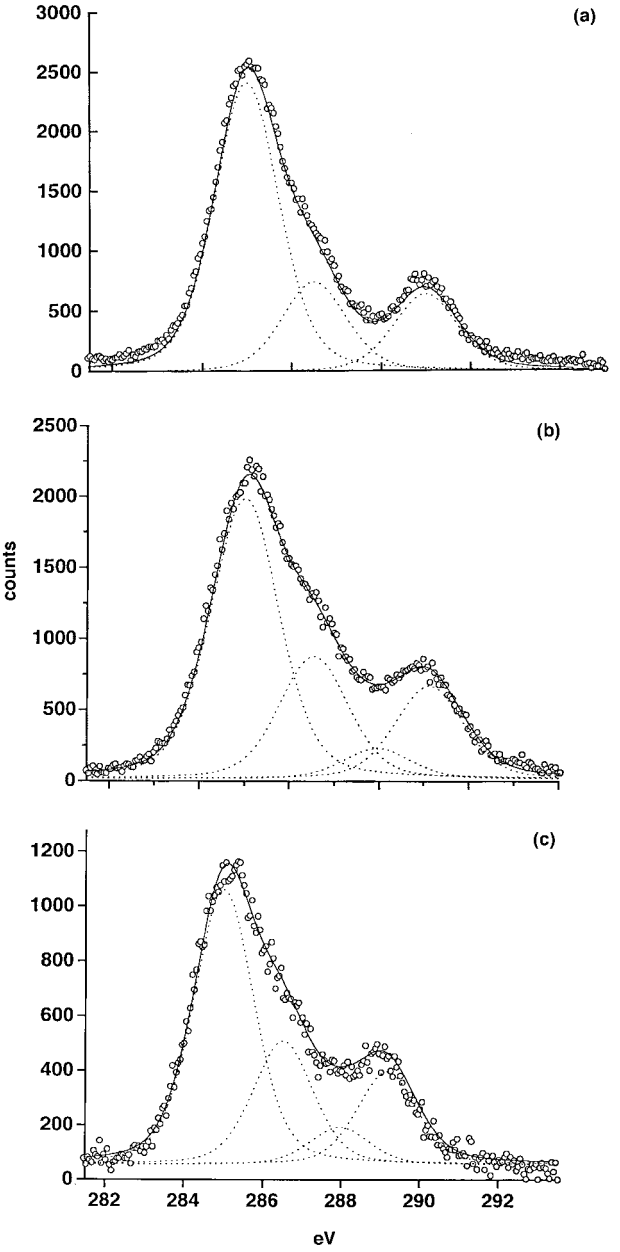


**Fig. 6** Fitted C 1s spectra of PET, untreated (a) and plasma-treated for 10 min (b) and 2 h (c).

appeared in the C 1s spectrum. Argon plasma treatment at either pressure studied increased the O:C ratio by a similar amount. Table 1 shows the O:C ratio as a function of treatment time for 0.1 mbar argon. Near-limiting values were obtained after 1 min treatment, after which only small changes to the lineshapes occurred and it reached a steady state by about 10 min. Survey scans showed that no nitrogen was present after plasma treatment.

### Lateral force microscopy

The plasma-modified Melinex 'O' and Mylar D surfaces were more easily disrupted by the motion of the tip during scanning (at the same applied load) than the untreated polymer. Lateral force imaging of untreated Melinex 'O' and Mylar D films showed only small frictional contrast on scanning in forward and reverse directions. After treatment with argon plasma there was a significant enhancement in the observed lateral force contrast. Lateral force images revealed greater detail of the structure of the surface additives on the plasma treated Mylar D surface (Fig. 7) although we have observed that the quality of images of the polymeric regions is poor in contact mode. Illustrative topography, lateral force images and friction loops (see below) of Mylar D and Melinex 'O' both plasma treated for 2 min are shown in Fig. 8 and 9. Friction loops have been constructed from line profiles and are shown for plasma-modified Melinex 'O' and Mylar D in Fig. 8(d) and 9(d) respectively. Fig. 10 shows the dependence of the frictional force on plasma treatment time for Melinex 'O' and over the additive features and the polymer surface for Mylar D. The frictional forces are larger over the polymer than the silicate additives in Mylar D. The difference in friction is much greater than on the untreated film. The maximum LFM signal is about seven times greater than that on the untreated Melinex 'O' and about five times that on the untreated Mylar D.

### Chemical force microscopy

Imaging plasma treated surfaces with AFM tips functionalised with a hydrophobic methyl-terminated alkanethiol monolayer led to some reduction in sample damage, which was more pronounced on surfaces which were treated for longer periods. Friction loops were constructed from images of plasma-treated Mylar D surfaces (or taken directly from the scope mode of the Nanoscope) with three chemically distinct types of 'Nanoprobe' AFM tips; (i) unmodified silicon nitride, (ii) methyl-terminated, (iii) carboxylic acid-terminated. It was found that the observed lateral forces did depend on the chemistry of the AFM tip, for both untreated and plasma-treated Mylar D surfaces, with the unmodified and carboxylic acid-modified tips having greater frictional interaction with the sample than the hydrophobic tips (Fig. 11). Table 2 shows relative frictional coefficients calculated from the slopes of friction *vs.* applied load plots. The change in lateral force signal on plasma treatment was much smaller than that obtained with the

**Table 1** XP data, O:C ratio as a function of treatment time (0.1 mbar argon)

| Treatment time/min | O:C[a] |
|---|---|
| 0 | 0.39 |
| 1 | 0.50 |
| 5 | 0.52 |
| 10 | 0.48 |
| 15 | 0.52 |
| 30 | 0.50 |
| 60 | 0.50 |
| 120 | 0.51 |

[a]Typical error in O:C ratio is $\pm 0.03$.

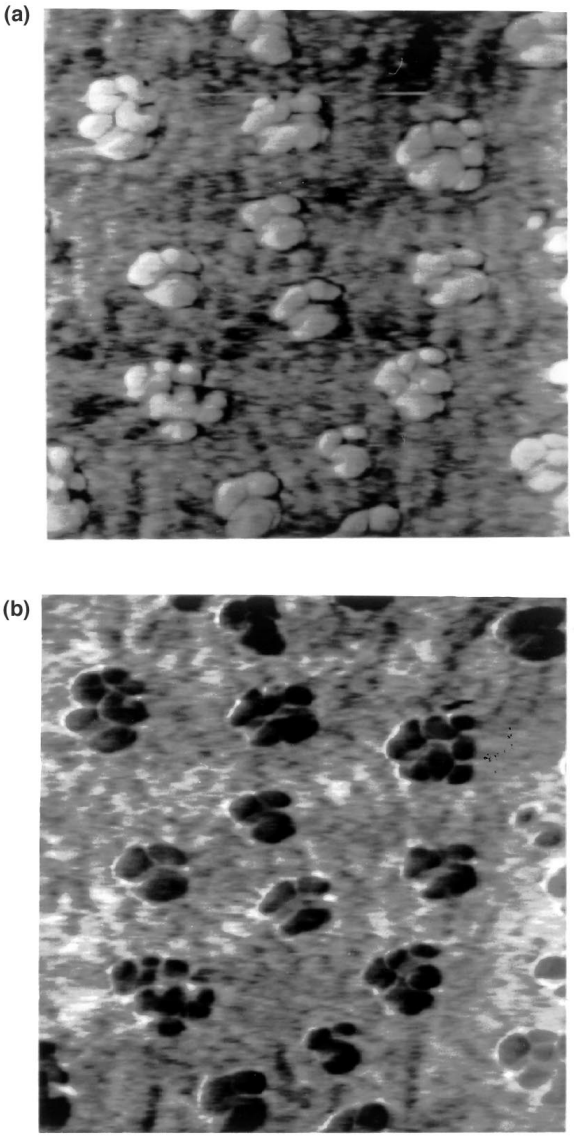


**Fig. 7** LFM images of Mylar D plasma treated for 10 s at 0.1 mbar. Images are forward (a) and reverse (b) directions. Z-scale ranges: (a) 1.66 to −2.55 nA; (b) 6.58–3.17 nA.

0.064 N m$^{-1}$ tips, as expected since the nanoprobes used to study the effect of tip chemistry were much stiffer laterally.

## Discussion

The main mechanisms currently thought responsible for the bondability improvement of plasma treated polymer surfaces are interfacial diffusion (aided by an increased molecular mobility caused by chain scission) and increased wettability.[30] The increased molecular mobility has been inferred from the observation that plasma treated polymers are bondable below their melting points.[30] The incorporation of polar functionalities should result in an improvement in the polymer wettability, and the data in Fig. 1 and 2 show much lower contact angles are obtainable for all the polar test liquids used following plasma treatment.

Surface free energy calculations for untreated Melinex 'O' by the method of van Oss and coworkers revealed a similar, but slightly higher, value ($\gamma_s \approx 47$ mN m$^{-1}$) than has been obtained in recent studies ($\gamma_s \approx 44$ mN m$^{-1}$).[29] Although the PET was obtained directly from sheets, nominally with clean sides facing inwards, it is possible that it may pick up some oleophilic impurities on exposure to atmosphere.[31] To test for contamination the polymer was sonicated in diethyl ether for

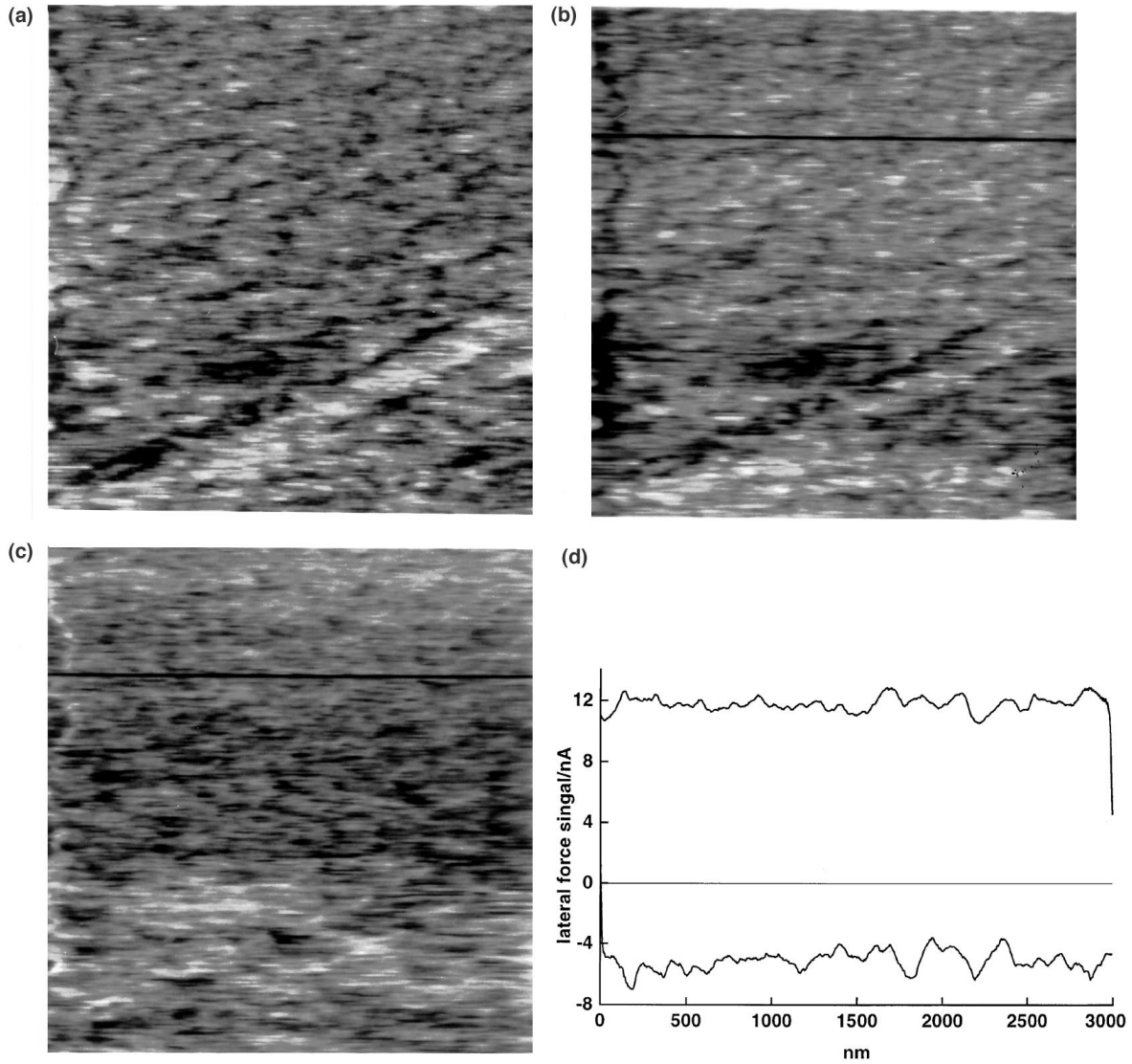


**Fig. 8** LFM images of Melinex 'O' plasma treated for 2 min at 0.1 mbar. Topographic (a) and lateral force images in forward (b) and reverse (c) directions. Friction loop (d) constructed from lateral force line profiles. Z-scale ranges: (a) 0–2 nm; (b) −1.74 to −9.28 nA; (c) 14.54–8.85 nA.

10 min and dried in high-purity nitrogen immediately before the contact angle measurements. The angles obtained were the same as those without the cleaning procedure; we conclude that the slight differences in wettability between our samples and others more likely reflect details of the polymer manufacture (such as surface roughness) rather than the presence of contamination. XPS showed the ratio of oxygen to carbon in the untreated film to be close (0.39) to the expected value (0.40), and a lack of obvious contamination.

Calculations of the variation in surface free energy after plasma treatment at 0.1 and 1.0 mbar argon are shown in Fig. 3 and 4 respectively. The total surface free energy obtained in this study is $64 \pm 2$ mN m$^{-1}$, after a period very much shorter than that required for the formation of the oriented, ridged structures reported in a previous study.[8] As expected from the contact angles, a significant increase in the polar component can be clearly seen. On plasma treatment the surface has acquired a pronounced acidic and more notably, basic character. Acidic interactions through formation of hydroxy and carboxyl groups on plasma treatment were expected,[7] and an enhancement in the acidic component of about 2 mN m$^{-1}$, very similar in magnitude to that calculated in the present study, has been reported in the argon plasma treatment of polycarbonate.[32] This was explained by the formation of phenolic hydrogen species, formed by photo-Fries rearrangements. The formation of phenolic species has been reported for corona discharge-treated PET by Briggs *et al.*[33] and these probably contribute to the increase in acidic interactions reported here.

The significant increase in basic interactions on the plasma-treated surface is notable. We suggest that the increase is due predominantly to the formation of carbonyl groups. XP spectra (see later) reveal a new peak which is attributed to the creation of carbonyl functions on the plasma-modified surface.[8,34] Carbonyl groups are thought to exhibit basic character[32] and Cueff *et al.* have reported XPS data showing that, for argon plasma treatment under their experimental conditions, the only carbon–oxygen functions to increase in intensity were carbonyl groups.[34] Nitrogen and oxygen plasma treatments of polypropylene have both been reported to produce a predominantly basic surface.[35,36] Whilst in the former case incorporation of basic N-containing functionalities is expected, in the latter a similar incorporation of carbonyl functions may be occurring.

van Oss, Chaudhury and Good have noted[24] that the occurrence of large basic components of the polar free energy (together with a much smaller $\gamma^+$ value) is not uncommon in polymers and natural compounds such as proteins. These are termed[24] 'monopolar surfaces', and PET is considered[27] to be a moderate $\gamma^-$ monopole. Strong hydrogen bonding in the depolymerised surface may increase the p$K_a$ of the acid groups formed on plasma treatment, leading to a decrease in the acid

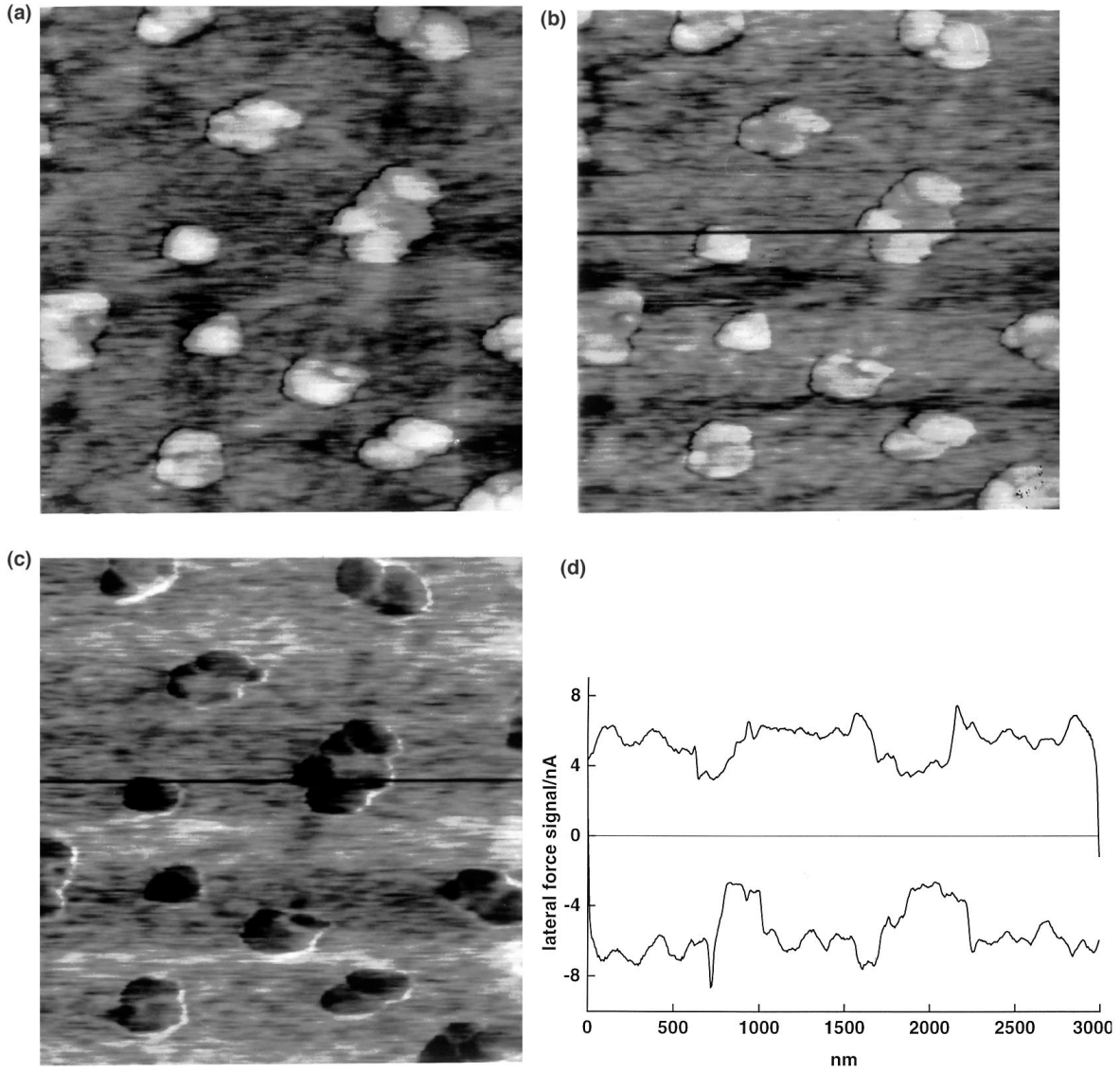


**Fig. 9** LFM images of Myler D plasma treated for 2 min at 0.1 mbar. Topographic (a) and lateral force images in forward (b) and reverse (c) directions. Friction loop (d) constructed from lateral force line profiles. Z-scale ranges: (a) 0–40 nm; (b) −1.33 to −11.11 nA; (c) 9.46–2.44 nA.

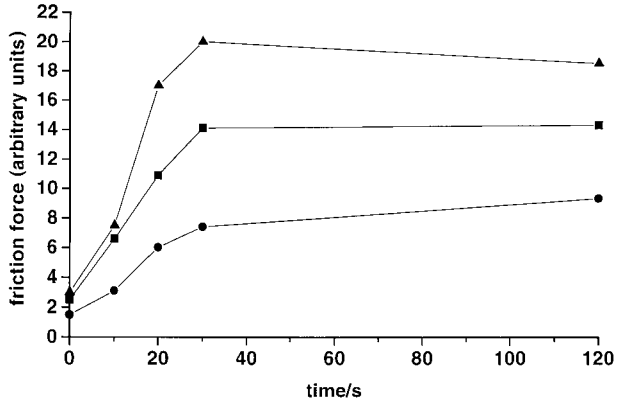


**Fig. 10** Variation in friction signal with treatment time. Melinex 'O' (▲), on polymer background of Mylar D (■), over additives on Mylar D (●).

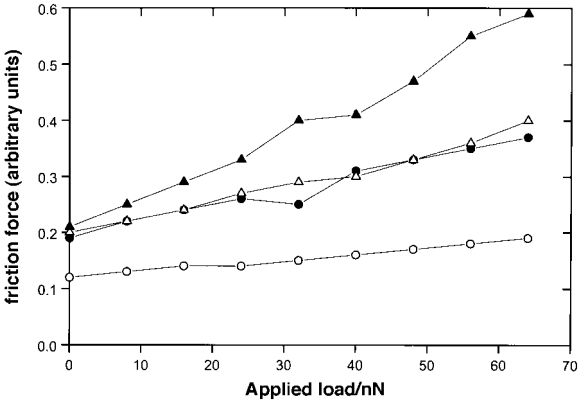


**Fig. 11** Variation of friction force with AFM tip chemistry for untreated Mylar D and plasma treated for 20 min at 0.1 mbar. Tip-sample combinations: unmodified-plasma treated (▲), unmodified-untreated (△), methyl-plasma treated (●), methyl-untreated (○).

component of the polar free energy. It should also be noted that the exact acidic and basic parameters are dependent on the values of the test liquid acid and base components chosen. A revised scale of the acid–base parameters of common solvents with $\gamma_w^+ = 65\ mN\ m^{-1}$ and $\gamma_w^- = 10\ mN\ m^{-1}$ has recently been proposed (previously van Oss and co-workers set $\gamma_w^+ = \gamma_w^- = 25.5\ mN\ m^{-1}$). The authors have suggested that the modified values may allow the acidic properties of polymers to be more correctly expressed.[37]

The similarity of water and glycerol contact angles on plasma-modified surfaces is notable. It has been reported that

**Table 2** Dependence of the relative friction coefficient over polymeric regions of Mylar D on the chemistry of the AFM tip

| Tip chemistry | Relative friction coefficient | |
|---|---|---|
| | Untreated polymer | After plasma treatment[a] |
| Silicon nitride | $0.20 \pm 0.02$ | $0.36 \pm 0.05$ |
| Methyl-terminated | $0.07 \pm 0.01$ | $0.23 \pm 0.05$ |
| Carboxylic acid-terminated | $0.21 \pm 0.04$ | $0.32 \pm 0.03$ |

[a]Plasma treatment for 20 min at 0.1 mbar. Errors shown are standard deviations of values from 3–10 separate determinations.

the contact angle of glycerol is virtually identical to that of water for a wide range of biological systems.[27] Differences in the relative acid–base parameters of the two liquids can account for the unexpected closeness of angles on two liquids whose surface tensions differ by 12%.[27] PET does not become completely wetted by either water or glycerol on argon plasma treatment. This is indicative of a maximum in surface energy. As suggested previously,[8–10] this is probably due to a steady-state being reached between functionalisation (polar group incorporation) and surface etching.

Comparison with data for diiodomethane shows that, surprisingly, the contact angle of the apolar liquid increases on exposure to plasma. We have previously shown[8] that plasma treated material is much more susceptible to tip-induced damage during scanning. We suggest that the observed increase in the contact angles with apolar liquids (indicative of a decrease in dispersive interactions between surface and test liquid) is related to surface disorder caused by plasma-induced chain-scission. The increase in surface mobility (disorder) is discussed further below in connection with the SFM data.

The contact angle measurements of test liquids on a solid polymer surface have also been used to calculate the thermodynamic work of solid–liquid adhesion, as illustrated in Fig. 5. The acid–base contribution to the work of adhesion increases on plasma treatment, as expected from the increase in surface free energy.[38] The increase in the acid–base component of the work of water–PET adhesion is greater than the corresponding increase in the work of formamide–PET adhesion. Since water is a much stronger acid than formamide the importance of basic interactions on the plasma-modified surface is clear.

As shown in Table 1, XPS reveals a substantial increase in the O : C ratio after plasma treatment and subsequent exposure to atmosphere. The O : C ratio is $0.50 \pm 0.03$ after 1 min treatment at 0.1 mbar argon and does not rise significantly thereafter. The magnitude of this increase is in agreement with a recent determination ($O:C \approx 0.51$–$0.56$) by France and Short[7] at 10 W and $2.5 \times 10^{-2}$ mbar argon using a similar reactor configuration. It has been considered[7–10] that plasma attack on the ester functionally would be likely to lead to chain scission, leading to etching and a relatively low saturation level for oxygen incorporation and a large amount of low molecular weight material.[7,9] By comparing the etching rates of several organic materials, Prat *et al.* have concluded that polymers containing functions such as ester groups are more susceptible to degradation since it can more easily occur by initial chain scission at the functional groups.[10] Indeed, there are reports of PET surface modification by argon plasma which show a small decrease in C–O and ester peak intensity.[34,39] It has been suggested that the breaking of ester bonds can lead to radicals that are resonance-stabilised over those formed in C–C bond breaking.[9] Under conditions where the authors reported a loss of ester oxygen, the only peak found to increase in intensity was a new species of *ca.* 3.0 eV higher binding energy than hydrocarbon.[34] These authors, and others,[7] have assigned this to the creation of isolated carbonyl groups.

Peak fitting to the C 1s lineshape, after plasma treatment has also revealed a new peak 3 eV from hydrocarbon in the present study (Fig. 6). The peak appears after only 1 min treatment in agreement with the rapid increase in basic interaction revealed by the contact angle data. Small changes in the C 1s lineshape do occur beyond this point, notably an increase in the carbonyl peak intensity; however the changes are smaller than those that occur in the first min of treatment and steady state is reached after 10 min. An exact correlation between the time-scales of the variations in contact angle and XP spectra is not expected due to the different sampling depths and hence differing surface selectivities of the two techniques: wettability is sensitive to the outer 0.5–1.0 nm of the surface[40] whilst XPS data contain contributions from a greater depth, *ca.* 5–10 nm.[19]

Fig. 7 shows lateral force images of the Mylar D surface after only 10 s exposure to plasma. While we have previously reported that plasma treated PET is disrupted during contact mode SFM,[8] the additive particles are imaged here with clarity. Some of the additive features are in fact aggregates of several smaller particles. After longer exposure this delineation of the additives became less clear, presumably because they were damaged by the plasma.

The contrast in LFM arises from twisting motions of the cantilever as it transverses the surface. These twisting motions arise from forces acting parallel to the plane of the sample surface. It is clear that frictional forces contribute to the LFM signal; however, when the local topography of the surface changes then the LFM signal may also contain contributions from normal (load) forces. Appendix 2 shows how the effects of normal forces on the frictional signal can be eliminated by scanning in forward and reverse directions. The images in Fig. 7 and 9 appear to indicate that an inversion of contrast occurs over the additives on reversing the scan direction, implying significant frictional interaction. However, examination of the friction loops of Mylar D plasma-treated for 2 min [Fig. 9(d)] reveals that the contrast inversion in the LFM image is illusory. Careful consideration of the line profiles shows that the lateral force over the additives changes little, while a large change is seen over the polymeric regions. The magnitude of the change is such that the relative contrast over the silicates changes in the image; however, the largest frictional interaction, according to the analysis of Grafström *et al.*[17] (see Appendix 2) is over the polymer. Friction loops have shown that the lateral force is constant over an image, suggesting that although the plasma-modified surface can be worn by the SFM tip during scanning the tip-induced topographic changes (which, in principle, could affect the friction measurement by making the subtraction inexact) are small. In an earlier paper[41] we observed a similar (although smaller) contrast inversion over the additive particles in untreated Mylar D. However a re-examination of the untreated material suggests that the inversion is illusory there too, and that, for untreated Mylar D, the largest friction interaction is on the polymer surface. Obviously, great care must be taken in the interpretation of image contrast in LFM.

For Mylar D, the contrast over the polymer background and over the additive surface both show a sharp initial increase with time of plasma treatment as shown in Fig. 10. The difference in friction between the additives and the polymeric background is much larger than on the untreated film. Illustrative topography, lateral force images and friction loops

of Mylar D and Melinex 'O' both plasma treated for 2 min are shown in Fig. 8 and 9. Comparison of the lateral force line profiles with the topographic image provides evidence that the lateral forces are affected by the local sample slope; the friction signal is clearly altered as the tip encounters the surface additives. However, the friction over the *central* regions of the additives and over the polymeric background is invariant across the image; the method of Grafström *et al.*[17] is applicable for surfaces of this roughness.

The data shown in Fig. 10 have all been recorded using the same SFM tip. Thus, although we do not know the exact lateral forces (as both the lateral spring constants of our tips and the sensitivity of our microscope to lateral displacements are not accurately known), the *relative* frictional forces are accurately ($\pm 10\%$) determined. After plasma treatment Melinex 'O' surface has a frictional response up to seven times greater than the virgin material. The surface friction measured by LFM reaches limiting values on closely similar time-scales to the wettability and XPS data.

If acid–base interactions between tip and sample are important in determining the frictional interaction then the measured friction force should vary with tip chemistry in the following order: acid-terminated tip $\geq$ unmodified silicon nitride tip $>$ methyl-terminated tip. Although the bulk composition of the unmodified tip is silicon nitride, it is thought that oxides and silanols are present at the surface yielding a polar tip.[42] Unmodified and COOH-terminated tips are known to show similar frictional characteristics when imaging SAMs in air.[43] Fig. 11 shows the variation in friction force with load for methyl-terminated and unmodified tips before and after plasma treatment for 20 min. It can be seen that for a given load, the friction force measured with the methyl terminated tip for the treated polymer is significantly higher than that measured with the same tip for the untreated polymer, but similar to the force measured for the treated polymer with a bare tip. From the slopes of such plots it is possible to determine a relative coefficient of friction for a specific tip–sample combination, and these data are plotted in Table 2 along with measurements for acid-terminated tips. Both polar (unmodified and carboxylic acid-modified) tips have greater frictional interaction with the polymeric samples than the hydrophobic (apolar) tips do. There was a noticeable improvement in resolution on imaging the plasma-treated samples with hydrophobic methyl-coated tips. These results indicate that polar interactions between tip and sample make a significant contribution to the friction force measured by LFM.

The frictional force of an adhesive contact is a function of the contact load (here kept constant), the area of contact and the surface free energies of the two surfaces. On plasma treated surfaces both an increase in surface free energy (shown by the improved wettability) and an increase in tip–sample contact area (treated surfaces are more easily disrupted by the motion of the tip during contact mode scanning) occur and are mediated *via* chain scission processes. Studies by Bar *et al.* on LFM and force modulation microscopy of self-assembled monolayers have shown the importance of packing density (and hence tip–sample contact area) in determining the contrast in LFM images on chemically identical regions, with sharp contrast observed between heptanethiol and octadecanethiol monolayers.[44] We have used LFM to probe the surface friction on regions of different hydrophobicity on photopatterned PET films and photopatterned SAMs.[45] Imaging under similar conditions led to considerably smaller observed LFM contrast between hydrophilic and hydrophobic regions on these surfaces than was observed here between treated and untreated polymers. This observation, together with measurements of frictional forces between single-component self-assembled monolayers,[45] suggests that the greater frictional contrast observed after plasma treatment is not entirely due to differences in wettability.

If acid–base interactions were solely responsible for the increase in friction following plasma treatment, the magnitude of the change would be significantly smaller when the apolar, methyl-functionalised tips were used. However, the magnitude of the frictional increase on plasma treatment was similar for all the tip chemistries used. Therefore it is clear that while chemical interactions contribute to friction following treatment, there is a substantial additional contribution, which we attribute to an increase in the tip–sample contact area as a consequence of the mechanical softening of the surface. The observed correlation between surface free energy, probed by wettability and XPS, and surface friction, probed by LFM, is a consequence of the fact that chain scission (leading to mechanical weakness in the surface layer) and polar group incorporation (leading to increasing surface energy) occur on a similar time scale, and are complementary aspects of the same physical process.

## Conclusion

The combination of lateral force microscopy, wettability, and X-ray photoelectron spectroscopy has been used to analyse changes at the film surface after plasma treatment of poly(ethylene terephthalate). Calculations on contact angle data with a combination of polar and non-polar liquids have shown that argon plasma treatment considerably enhances the work of solid–(polar) liquid adhesion and the surface free energy of the films. This is shown to be due to the creation of acidic and basic functions on the polymer surface. This is confirmed by XP spectra which show an increased oxygen:carbon ratio after plasma treatment. In contrast, the Lifshitz–van der Waals (apolar) interactions decrease as a consequence of plasma-induced chain-scission. Friction force microscopy has shown that plasma-modified surfaces exhibit substantially higher friction than untreated material and are more easily disrupted by the movement of the tip during scanning. Typically, modified surfaces show a maximum frictional response which is about seven times higher than untreated material when imaging with the less stiff cantilevers. Friction forces on plasma-treated and unmodified Mylar D depend on the surface chemistry of the AFM tip. There is a correlation, on plasma treatment, between the rapid increases in surface friction probed by lateral force microscopy and surface free energy probed by wettability and X-ray photoelectron spectroscopy. Increased surface disorder and polar group incorporation both result from scission of polymer chains and contribute to the increase in friction.

## Acknowledgements

The authors are grateful to the EPSRC (grant GR/K/88071), the Royal Society and the Society of Chemical Industry for financial support. J.S.G.L. thanks the EPSRC for a research studentship. G.J.L. thanks the Nuffield Foundation for a Science Research Fellowship. The authors would like to thank the Department of Materials Engineering and Materials Design, University of Nottingham, where some of this work was carried out, and acknowledge the assistance of J. C. Bussey (University of Nottingham) in obtaining some of the XPS spectra. The authors are most grateful to Dr J. H. Clint (Surfactant Science Group, School of Chemistry, University of Hull) for supplying copies of his programs to obtain surface free energy data from contact angles and for useful discussions, and to Dr R. D. Short (University of Sheffield) for his assistance in designing the plasma reactor. The authors would also like to thank Professor D. Briggs (ICI, Wilton) for supplying Melinex 'O' with known orientation and for helpful and stimulating discussion.

## Appendix 1: Theory and calculation of surface free energies from contact angles

Contact angle measurements of liquids on a solid surface can be used to calculate the thermodynamic work of solid–liquid adhesion according to the Young–Dupré equation, [$W_{sl} = \gamma_l(1+\cos\theta)$]. The acid–base contribution to the work of adhesion can be separated[30,46] from the Lifshitz–van der Waals interactions:

$$W_{sl}^{total} = W_{sl}^{LW} + W_{sl}^{AB}$$

LW represents the sum of the three electrodynamic interactions which decay with distance at the same rate (primarily the London [dispersion] force, with small contributions from the Keesom dipole–dipole [orientation] and Debye dipole–induced dipole [induction] force), collectively designated[24,26] as Lifshitz–van der Waals ('apolar') interactions. AB represents the polar or acid–base interactions. Similarly, it has recently been established[24,26–29] that the surface free energy of the solid can be separated into two terms:

$$\gamma_s^{total} = \gamma_s^{LW} + \gamma_s^{AB}$$

A geometric mean approach can be used to determine the apolar component of the solid free energy from the contact angle of an apolar test liquid providing that the liquid is of high enough surface tension that it does not spread completely over the solid surface.[24,26–29] However, such an approach is flawed when considering the polar component.[29,38] Instead, several authors[35,36,38] have suggested the approach of van Oss, Chaudhury and Good[24,26–29] is the most useful in the investigation of acid–base properties of plasma-modified polymer surfaces. Van Oss *et al*. have introduced the concept of surface tension parameters, $\gamma^+$ and $\gamma^-$, due to acidic and basic functionalities respectively.[24] These comprise (non-additively) the polar surface free energy of a material *i*, ($\gamma_i^{AB}$), thus:

$$\gamma_i^{AB} = 2(\gamma_i^+\gamma_i^-)^{1/2}$$

The key to the modification of the Young's equation (below) proposed by these authors is the realisation that acidic functions in the test liquid interact with only basic functionalities on the solid surface and *vice versa*.

$$(1+\cos\theta)\gamma_l = 2[(\gamma_s^{LW}\gamma_l^{LW})^{1/2} + (\gamma_s^+\gamma_l^-)^{1/2} + (\gamma_s^-\gamma_l^+)^{1/2}]$$

In this Lifshitz–van der Waals/acid–base approach there are three unknown values for the surface tension components. When contact angle measurements are carried out with three or more liquids (at least two of which are polar) with known $\gamma^{LW}$, $\gamma^+$ and $\gamma^-$ values, a standard least-squares method can be used to solve for the three unknown parameters.[29]

## Appendix 2: Construction of friction loops to determine surface friction

A line profile of the forward and reverse scans, a friction loop, can be used to determine the frictional interaction between tip and sample according to the treatment of Grafström *et al.*[17] These authors have shown that for a force ($F_N$) normal to the sample due to the application of a load during imaging, the lateral force ($F_y$) in a direction *y* orthogonal to both the cantilever and surface normal is given by

$$F_y = F_{ty} - s_y F_N$$

where $s_y$ is the slope in the *y*-direction and $F_{ty}$ is the force tangential to the surface normal in the *y*-direction. When there are substantial variations in surface topography the $s_y F_N$ component can become significant. Since the lateral force is determined from the difference between signals reaching the left and right halves of a four-segment photodetector, in principle ignoring piezoelectric drift) the topographic contribution to the LFM image may be removed by subtracting images recorded in the forward and reverse directions. These comparisons of forward and reverse scans are often called friction loops and should reflect the frictional force acting between tip and sample.[16]

## References


1 E. M. Liston, L. Martinu and M. R. Wertheimer, *J. Adhes. Sci. Technol.*, 1993, **7**, 1091.
2 E. M. Liston, in *The Interfacial Interactions in Polymer Composites*, ed. G. Akovali, Kluwer Academic, London, 1993, p. 223.
3 A. M. Mayes and S. K. Kumar, *MRS Bull.*, 1997, **22**, 43.
4 F. D. Egitto and L. J. Matienzo, *IBM J. Res. Dev.*, 1994, **38**, 423.
5 K. Harth and H. Hibst, *Surf. Coat. Technol.*, 1993, **59**, 350.
6 F. Denes, *TRIP*, 1997, **5**, 23.
7 R. M. France and R. D. Short, *J. Chem. Soc., Faraday Trans.*, 1997, **93**, 3173.
8 B. D. Beake, J. S. G. Ling and G. J. Leggett, *J. Mater. Chem.*, 1998, **8**, 1735.
9 F. Clouet and M. K. Shi, *J. Appl. Polym. Sci.*, 1992, **46**, 1955.
10 R. Prat, M. K. Shi and F. Clouet, *J. Macromol. Sci–Pure Appl. Chem. A*, 1997, **34**, 471.
11 *Acid–Base Interactions, Relevance to Adhesion Science and Technology*, ed. K. L. Mittel and H. R. Anderson, Jr, VSP, Utrecht, 1991.
12 J. A. McLaughlin, D. Macken, B. J. Meenan, E. T. McAdams and P. D. Maguire, *Key Eng. Mater.*, 1995, **99–100**, 331.
13 J. F. Friedrich, W. Unger, A. Lippitz, T. Gross, P. Rohrer, W. Saur, J. Erdmann and H-V. Gorsler, *J. Adhes. Sci. Technol.*, 1995, **9**, 575.
14 A. Ringenbach, Y. Jugnet and Tran Minh Duc, *J. Adhes. Sci. Technol.*, 1995, **9**, 1209.
15 P. Gröning, M. Collaud, G. Dietler and L. Schlapbach, *Vide Couches Minces*, 1994, **272SS**, 140.
16 R. Overney and E. Meyer, *MRS Bull.*, 1993, **18**, 26.
17 S. Grafström, M. Neitzert, T. Hagen, J. Ackermann, R. Neumann, O. Probst and M. Wörtge, *Nanotechnology*, 1993, **4**, 143.
18 A. Noy, C. D. Frisbie, L. F. Rozsnyai, M. S. Wrighton and C. M. Lieber, *J. Am. Chem. Soc.*, 1995, **117**, 7943.
19 *Practical Surface Analysis*, ed. D. Briggs and M. Seah, 2nd edn. Wiley, 1990, vol. 1, p. 635.
20 G. Haugstad, W. L. Gladfelter, E. B. Weberg, R. T. Weberg and R. R. Jones, *Langmuir*, 1995, **11**, 3473.
21 J. A. Hammershmidt, B. Moasser, W. L. Gladfelter, G. Haugstad and R. R. Jones, *Macromolecules*, 1996, **29**, 8996.
22 E. W. van der Vegte and G. Hadziioannou, *Langmuir*, 1997, **13**, 4357.
23 C. D. Bain, E. B. Troughton, Y.-T. Tao, J. Evall, G. M. Whitesides and R. G. Nuzzo, *J. Am. Chem. Soc.*, 1989, **111**, 321.
24 C. J. van Oss, M. J. Chaudhury and R. J. Good, *Adv. Colloid Interface Sci.*, 1987, **28**, 35.
25 The computer programs used to obtain surface free energy data from contact angles were from Dr J. H. Clint (University of Hull).
26 C. J. van Oss, M. J. Chaudhury and R. J. Good, *Chem. Rev.*, 1988, **88**, 927.
27 C. J. van Oss, M. J. Chaudhury and R. J. Good, *Langmuir*, 1988, **4**, 884.
28 C. J. van Oss, *Colloids Surf. A: Physico. Eng. Asp.*, 1993, **78**, 1.
29 W. Wu, R. F. Giese, Jr. and C. J. van Oss, *Langmuir*, 1995, **11**, 379.
30 *Polymer Interface and Adhesion*, ed. S. Wu, Marcel Dekker, New York, 1982, pp. 298–321.
31 Prof. D. Briggs, personal communication.
32 S. Vallon, B. Drévillon, F. Poncin-Epalliard, J. E. Klemberg-Sapieha and L. Martinu, *J. Vac. Sci. Technol. A*, 1996, **14**, 3194.
33 D. Briggs, D. G. Rance, C. R. Kendall and A. R. Blythe, *Polymer*, 1980, **21**, 895.
34 R. Cueff, G. Baud, J. P. Besse, M. Jacquet and M. Benmalek, *J. Adhes.*, 1993, **42**, 249.
35 J. Behnisch, A. Holländer and H. Zimmermann, *Int. J. Polym. Mater.*, 1994, **23**, 215.
36 J. Behnisch, A. Holländer and H. Zimmermann, *J. Appl. Polym. Sci.*, 1993, **49**, 117.
37 C. Della Volpe and S. Siboni, *J. Colloid Interface Sci.*, 1997, **195**, 121.
38 N. Shahidzadeh-Ahmadi, F. Arefi-Khonsari and J. Amouroux, *J. Mater. Chem.*, 1995, **5**, 229.

39 Q. T. Le, J. J. Pireaux and J. J. Verbist, *Surf. Interface Anal.*, 1994, **22**, 224.
40 P. E. Laibinis, C. D. Bain, R. G. Nuzzo and G. M. Whitesides, *J. Phys. Chem.*, 1995, **99**, 7663.
41 J. S. G. Ling and G. J. Leggett, *Polymer*, 1997, **38**, 2617.
42 J. M. Williams, T. Han and T. P. Beebe, Jr., *Langmuir*, 1996, **12**, 1291.
43 J.-B. D. Green, M. T. McDermott, M. D. Porter and L. M. Siperko, *J. Phys. Chem.*, 1995, **99**, 10960.
44 G. Bar, S. Rubin, A. N. Parikh, B. I. Swanson, T. A. Zawodzinski, Jr. and M.-H. Whangbo, *Langmuir*, 1997, **13**, 373.
45 B. D. Beake and G. J. Leggett, unpublished work.
46 X. Qin and W. V. Chang, *J. Adhes. Sci. Technol.*, 1996, **10**, 963.

*Paper 8/07261B*